Integration
geoscience
engineering
partnership
geoConvention 2013

Multi-component or vector dip filtering using the S-transform

Kristof De Meersman, CGGVeritas, Calgary, Canada
kristof.demeersman@cggveritas.com
and
Majda Mihoub, CGGVeritas, Massy, France

Summary

In this work we combine principles of vector (multi-component) processing with those of conventional dip filters in a way that handles irregular spatially sampled data as well as non-stationarity in time and frequency. The result is a method to estimate the dominant local (in time, frequency and spatial coordinates) polarization and dip properties in multi-component seismic data. We then adapt this method to create a multi-component dip filter that removes unwanted ground roll noise from the data. Local dip is estimated using data from all 3 components simultaneously. If noise dips are detected, a 3C estimate of the noise is calculated and subtracted from the data. Our filter is tested on a realistic 3C synthetic with dispersive elliptically polarized surface wave noise in the presence of PP and PS reflections and random background noise.

Introduction

Geophysicists have access to a multitude of tools to attenuate surface wave noise. Most of these tools exploit lateral coherency between groups of traces - so called dip filters. Examples of these filters include FK, FX, radon, rank reduction and any 3D extension of the above. The advent of multi-component data also led to the development of vector-type filters that utilize polarization properties to distinguish signal and noise using all recorded components. Unfortunately, many of these techniques have in common that they poorly handle non-stationarity. Any frequency domain filter typically does not recognize that the frequency content of seismic signal and noise changes with time. It assumes time domain stationarity. And, likewise any time-domain ('sliding window') filter typically ignores that signal and noise properties change as a function of frequency. It assumes stationarity in the frequency domain. Here, we lay out the framework for vector (multi-component) dip filtering that handles non stationary naturally in both the time and frequency domain. In short, we estimate the local (in time, frequency and space) polarization and dip properties of the data and use this information to remove unwanted signals.

Theory: Vector dip estimation and filtering in the S-domain

Central to our method is a data transform that provides time variant spectral estimates. While many such transforms are available in the literature we chose the S-transform for a number of reasons that we will explain next (Stockwell et al., 1996). The S-transform is closely related –and could be considered the ultimate extension of - the short-time Fourier transform and the Gabor transform. It also shares many properties with wavelet transforms. The main difference is that the wavelet transform works in scales as opposed to frequencies and that it does not provide absolute phase information (Brown et al., 2010). Absolute phase infromation is desirable when designing dip filters for irregularly spatially sampled data. Like the Gabor transform, the S-transform uses a Gaussian window to localize the spectral information. Contrary to the Gabor transform however, the S-transform does not use a fixed Gaussian window for all frequencies, but one that scales as a function of frequency. As such it aims to achieve an optimal balance between temporal and frequency resolution. Shorter Gaussian

windows are used to estimate the amplitude and phase of higher frequencies while longer Gaussian windows are used to estimate the low frequency properties of the data. The continuous definition of the S-transform ***S****(τ,f)* of a time series *s(t)* is given by:

$$\mathbf{S}(\tau,f)=\int_{-\infty}^{\infty}\frac{|f|}{\sqrt{2\pi}}e^{\left(-\frac{f^2(\tau-t)^2}{2}\right)}s(t)e^{(-2\pi ift)}dt \qquad (1)$$

The scalar and the real exponent in this equation define the Gaussian window and the complex exponent is simply the Fourier kernel. The S-transform has a number of desirable properties that make it particularly useful for the purpose of multi-component or vector dip filtering. First, it is easily invertible. Integrating or summing ***S****(τ,f)* over the time axis will yield the Fourier spectrum ***F****(f)* of the input signal. So one easy way to implement filtering in the S-domain is to omit or zero out samples in the integration so that the resulting Fourier spectrum is void of information from the unwanted signal. A more complete and relevant description of filtering options in the time-frequency domain can be found in Margrave (1998). Second, any time-slice of the S-transform behaves exactly like a Fourier transform. So, in principle any FX(Y) type dip filter can be modified to handle non-stationary simply by replacing the input Fourier spectrum with a time slice of the S-transform. Third, Pinnegar (2006) demonstrated it is possible to perform polarization (vector) filtering in the S-domain so that an extension to vector dip filtering becomes fairly straight forward. Finally, while it can be computationally expensive to compute the S-transform and filter in this domain, Brown et al. (2010) introduced a sampling scheme that significantly reduces computational costs, especially for low-frequency noise problems. So basically, everything that is required to achieve computationally efficient vector dip filtering in the time-frequency domain is well documented in the literature and one only needs to put the different techniques together.

To describe our vector dip filter we start by defining the a local data-matrix ***D*****(x,f,τ)**. This 3 by N matrix contains S-transform spectral estimates $\mathbf{S}(\tau,f)$ for a chosen time (τ) and frequency (*f*) and for all three components (*r, t* and *z*) of N selected traces (*x*). The trace at the center of the matrix is the one for which the dominant local dip will be estimated and all N-1 other traces that make up ***D*** are selected from within a shot or receiver gather or cross spread. N is typically between 3 and 21 and traces are selected from within the vicinity of the trace at the center and which is denoted by the subscript *c*. We work in polar coordinates (offset-azimuth) so that our definition of ***D*** applies to both 2D and 3D gathers. We also assume that traces in ***D*** are sorted by increasing offset:

$$\mathbf{D}=\begin{bmatrix}\mathbf{d}_r\\ \mathbf{d}_t\\ \mathbf{d}_z\end{bmatrix}=\begin{bmatrix} d_{r1}e^{-j\varphi_{r1}} & \cdots & d_{rc}e^{-j\varphi_{rc}} & \cdots & d_{rn}e^{-j\varphi_{rn}}\\ d_{t1}e^{-j\varphi_{t1}} & \cdots & d_{tc}e^{-j\varphi_{tc}} & \cdots & d_{tn}e^{-j\varphi_{tn}}\\ d_{z1}e^{-j\varphi_{z1}} & \cdots & d_{zc}e^{-j\varphi_{zc}} & \cdots & d_{zn}e^{-j\varphi_{zn}}\end{bmatrix} \qquad (2)$$

Next we cross correlate the last N-1 columns of ***D*** with the first N-1 columns to obtain:

$$\mathbf{X}=\begin{bmatrix} d_{r_1}d_{r_2}e^{-j\Delta\varphi_{r_{2,1}}} & \cdots & d_{r_{n-1}}d_{r_n}e^{-j\Delta\varphi_{r_{n,n-1}}}\\ d_{t_1}d_{t_2}e^{-j\Delta\varphi_{t_{2,1}}} & \cdots & d_{t_{n-1}}d_{t_n}e^{-j\Delta\varphi_{t_{n,n-1}}}\\ d_{z_1}d_{z_1}e^{-j\Delta\varphi_{z_{2,1}}} & \cdots & d_{z_{n-1}}d_{z_n}e^{-j\Delta\varphi_{z_{n,n-1}}}\end{bmatrix} \qquad (3)$$

The phase angles $\Delta\varphi$ contain information on the velocity and this information can be extracted from $\boldsymbol{X}$ in various ways. Here, we propose a very simple approximation assuming a single local dip in the presence of background noise. This is reasonable given that $\boldsymbol{X}$ relates to a localized portion of the data: a specific frequency, time and spatial coordinate. If surface wave noise is present we assume it is the dominant signal and hence, most of the energy in $\boldsymbol{X}$ will be related to the noise. If no surface waves are present then $\boldsymbol{X}$ will be dominated by velocity information from reflected energy. The phase angles $\varphi_{i+1,i}$ are a function of the offset difference $\Delta x_{i+1,i}$ and the local angular wave number $k_{i+1,i}$ so that $\varphi_{i+1,i}=k_{i+1,i}\,\Delta x_{i+1,i}$. We do not assume regular spatial sampling so that the offset differences $\Delta x_{i+1,I}$ are allowed to vary between columns of $\boldsymbol{X}$. The wave number relates to local velocity V through: $V=2\pi f k^{-1}$. The local velocity can thus be recovered from the average angular wave number which is:

$$\bar{k} = \arctan\left(\frac{\sum_{r,t,z}\sum_{i}\sin(k_{i+1,1})}{\sum_{r,t,z}\sum_{i}\cos(k_{i+1,1})}\right) \quad (4)$$

Note that our definition uses three components (*r, t* and *z*), but in principle it is valid for any number of components, including conventional 1C data. It is also possible to assign weights to the sine and cosine terms. For example, if these weights are derived from the amplitude terms *d* for each component then this will effectively reduce the importance of the transverse component in the averaging. This would be desirable considering that the transverse component typically contains very little coherent signal and noise. Figure 1 shows a synthetic data example where we demonstrate the ability of our method to estimate local dip. The left panel in Figure 1 shows linear dips computed using a 3D shot gather with 50 m receiver spacing and 180 m receiver line spacing. A bandpass filter with corner frequencies of 2,3,7,9 Hz was applied. The middle panel shows the 5Hz S-transform amplitude spectrum of the data. The panel on the right shows the local (instantaneous) velocity at 5Hz. The data window is 9 traces long, effectively making this a 2D receiver line estimate.

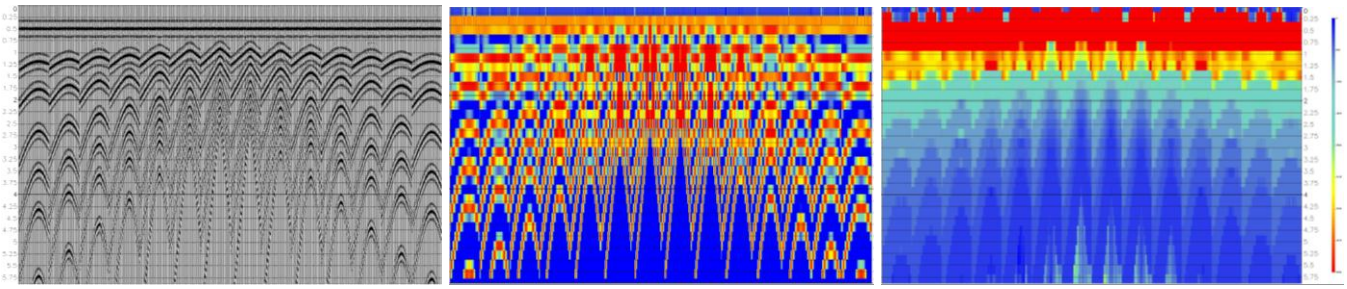

Figure 1

Figure 1: (Left) synthetic seismic data consisting of 8 linearly dipping events with 5Hz center frequency computed using a real 3D shot geometry with 50 m receiver spacing and 180 m receiver line spacing. The modeled linear events are sampled at 2ms and have intercepts and velocities of 500ms-Infinite, 900ms-4000 m/s, 1200ms-2000 m/s, 1500ms-1000 m/s, 1750ms-666 m/s, 2000ms-500 m/s and 2250ms-333 m/s. (Middle) S-transform 5Hz amplitude spectrum sampled at 200ms (1 period). (Right) 5Hz local velocity estimate derived from the 5Hz S-transform spectrum using Equation 4. The color map ranges between 0m/s (blue) and 5000m/s (red). All velocities can be recovered except that of the 333 m/s event due to severe spatial aliasing (more than ½ period) at a 50m station interval.

Now that the local velocity is known we can use this to estimate the vector ***v*** through slant stacking. To do this we multiply the data-matrix ***D*** with a dip-steering vector $\mathbf{s}_{\bar{k}}$ and obtain:

$$\mathbf{v} = \mathbf{D}\mathbf{s}_{\bar{k}} = \begin{bmatrix} d_{r1}e^{-j\varphi_{r1}} & \cdots & d_{rc}e^{-j\varphi_{rc}} & \cdots & d_{rn}e^{-j\varphi_{rn}} \\ d_{t1}e^{-j\varphi_{t1}} & \cdots & d_{tc}e^{-j\varphi_{tc}} & \cdots & d_{tn}e^{-j\varphi_{tn}} \\ d_{z1}e^{-j\varphi_{z1}} & \cdots & d_{zc}e^{-j\varphi_{zc}} & \cdots & d_{zn}e^{-j\varphi_{zn}} \end{bmatrix} \left[e^{-j\bar{k}(x_1 - x_c)} \quad \cdots \quad 1 \quad \cdots \quad e^{-j\bar{k}(x_n - x_c)} \right]^H \quad (5)$$

H denotes the Hermitian or complex conjugate transpose. If we assume that there are no variations in noise amplitude with offset then the elements in ***v*** can serve as estimates for the 3C trace at the center of D. The amplitude $\bar{d}_{zc}$ and phase $\bar{\varphi}_{zc}$ of the element in ***v*** that corresponds to the vertical component would serve as an estimate for the trace at the center of D. To accommodate amplitude variations with offset we can choose to retain only the phase of ***v*** and compute the least-squares estimates of the amplitudes $\bar{d}_c$ for the trace at the center. For the vertical component we get $\bar{d}_{zc} = d_{zc}\cos(\varphi_{zc} - \bar{k}x_{zc} - v_z)$ so as to minimize $\left|\bar{d}_{zc}e^{-j\bar{\varphi}_{zc}} - d_{zc}e^{-j\varphi_{zc}}\right|^2$. This is the least squares error between the estimated and observed spectral sample. Similar expressions can be derived for the radial and transverse components.

We have also implemented an alternative approach to estimating local dip (velocity) and polarization properties and which involves computing the singular value decomposition (SVD) of the data matrix **D**. The left singular vectors can be interpreted as polarization vectors while the right singular vectors can be used to obtain local velocity estimates. Note that **X** in equation (3) would simply reduce to a 1 *by* n-1 vector when applied to the right singular vectors. One advantage of using the SVD approach is that it effectively decomposes **D** into the superposition of 3 (in the case of 3C data) independent signals that can be analyzed separately. This would increase our ability to separate the dominant surface wave noise signal from additive reflection and random noise energy in **D**.

Examples

To test our method we generated a synthetic 3D 3C shot gather using the same geometry as that used for Figure 1. The vertical component contains 4 P-wave reflection events (4Hz–40Hz) while the radial component contains an equal number of PS reflection events (4Hz–25Hz). Elliptically polarized dispersive ground roll (3Hz-10Hz, 500m/s – 800m/s) is modeled on the vertical and radial components and random noise is added to all three components (Figure 2). The ground roll noise estimates obtained for each component and using the least squares method described in this abstract are shown in Figure 3. Our filter operated in the frequency band defined by a 1Hz-2Hz-12Hz-17Hz Ormsby filter and removed noise with velocities between 300m/s and 1000m/s. Subtracting the noise estimates in Figure 3 from the data in Figure 2 results in the filtered data in Figure 4. While some residual ground roll can be observed the PP and PS reflection signal remains largely untouched. We anticipate that the filtering could be improved upon further using adaptive subtraction. The residual ground roll is a direct consequence of our least squares estimation of the noise which is aimed at preserving reflection signal at the cost of missing some portion of the coherent noise. Figure 5 contains the local dominant velocity estimates that were used by the filter to estimate the noise. Velocities for frequencies of 5Hz, 7Hz and 9Hz are shown. The colors range between 200m/s (blue) and 1100m/s (red). The ground roll is typically identifiable by colors ranging from green-yellow-orange. Velocities related to reflection signal are typically identifiable as red whereas random noise appears mainly in blue. Comparing velocities from different frequencies clearly shows the dispersive nature of the coherent noise.

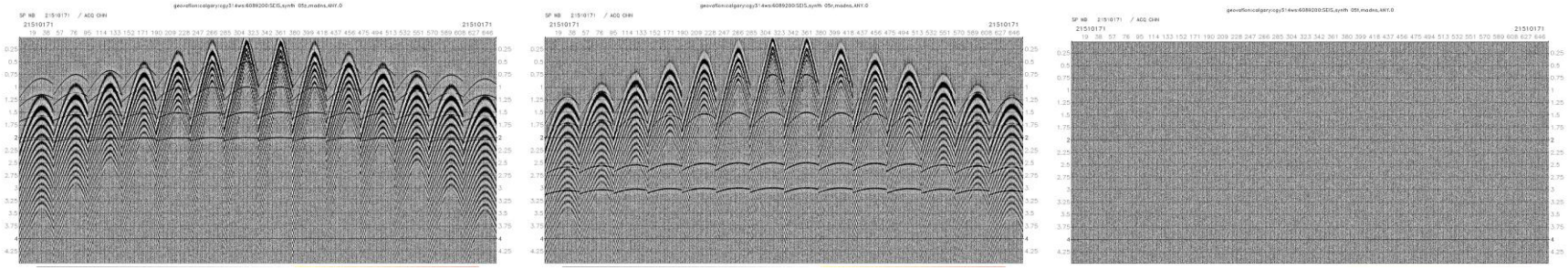

Figure 2: Synthetic 3D 3C shot gather with coherent dispersive ground roll and random noise. (Left) The vertical component contains 4 P-wave events in the presence of coherent and random noise. (Middle) The radial component contains 4 PS-wave events in the presence of coherent and random noise. The ground roll elliptically polarized. (Right) The transverse component contains random background noise only.

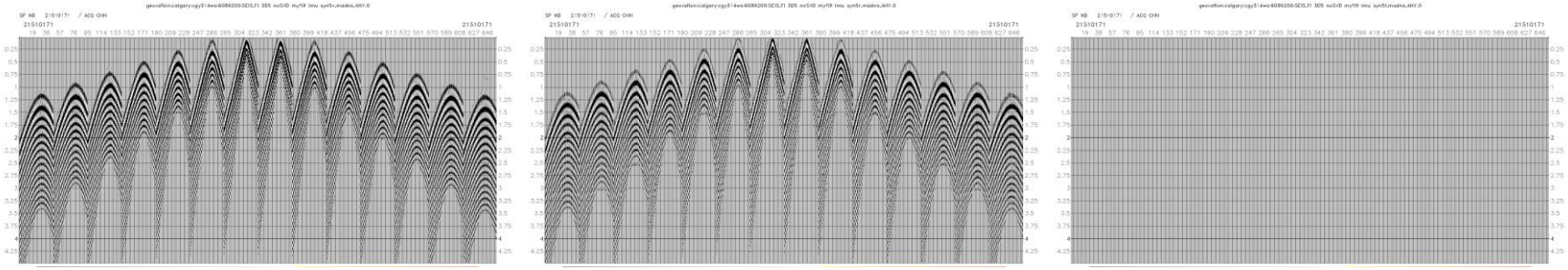

Figure 3: Noise estimates for the Vertical (left), Radial (middle) and Transverse (right) components. Even though strong 3C noise is detected the polarization properties of that noise are correctly predicted which is evident from the lack of significant predicted noise on the transverse (right).

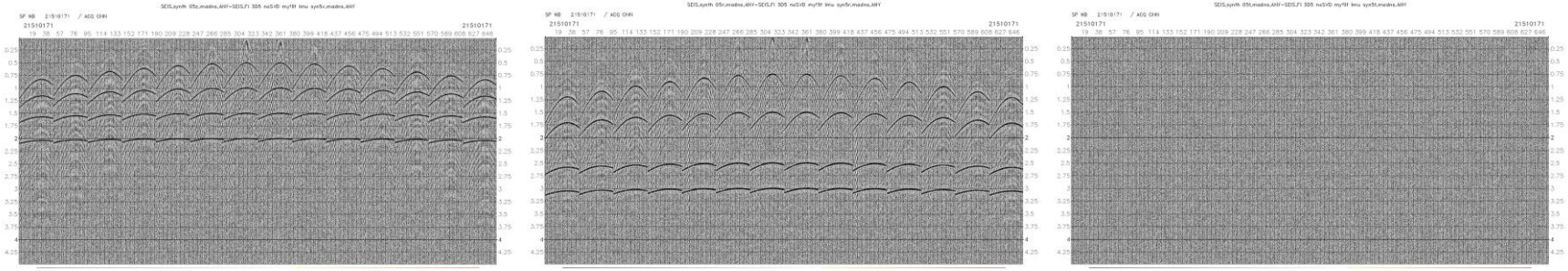

Figure 4: Filtered vertical (Left), Radial (Middle) and Transverse (Right) data. These results are obtained after direct subtraction of the data in Figure 2 and the noise in Figure 3.

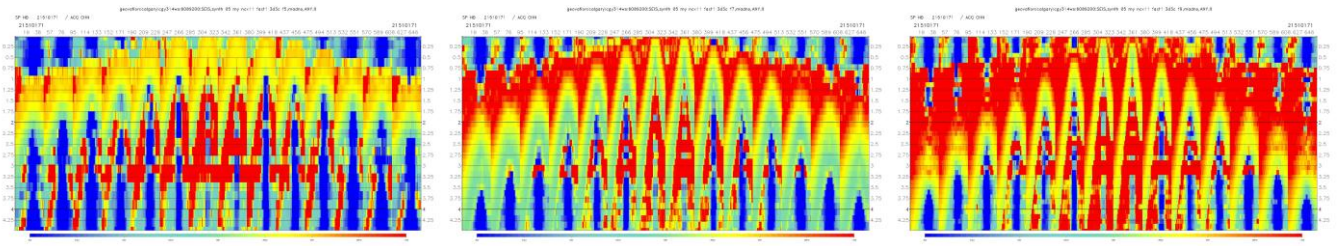

Figure 5: Instantaneous, local 3C velocity estimates calculated by our filter and used to model the noise. Velocity estimates for frequencies of 5Hz, 7Hz and 9 Hz are shown. The color bar ranges between 200m/s (blue) and 1100m/s (red). The ground roll is clearly identifiable by colors ranging from green (600m/s) over yellow (800m/s)

Conclusions

In this paper we introduce the concepts multi-component vector dip filtering in the time-frequency domain. The resulting filter can handle any number of recorded components, non-stationary and dispersive noise and estimates frequency dependent local (in time and spatial coordinate) velocity estimates. Encouraging results are obtained when testing this filter on a realistic 3C synthetic with dispersive elliptically polarized surface wave noise in the presence of PP and PS reflections and random background noise. We have also tested the method on real data with encouraging results and for which show rights are pending.

Acknowledgements

The authors would like to thank CGGVeritas for the permission to publish this paper. Many thanks also to Richard Wombell, Daniel Trad, Bruno Gratacos and Scott Haffner for reviewing.

References

Brown, R.A, Lauzon, M.L. and Frayne, R., A general description of linear time-frequency transforms and formulation of a fast, invertible transform that samples the continuous S-transform spectrum nonredundantly: IEEE Transactions on Signal Processing, (2010) 58(1).

Margrave, G., Theory of nonstationary linear filtering in the Fourier domain with application to time-variant filtering: geophysics (1998), 63(1), 244–259.

Pinnegar, C. R., Polarization analysis and polarization filtering of three-component signals with the time–frequency S-transform: Geophys. J. Int. (2006) 165, 596–606.

Stockwell, RG, L Mansinha, and RP Lowe (1996). Localization of the complex spectrum: the S-transform, IEEE Transactions on Signal Processing 44 (4), p 998-1001.